An Intrinsic Geometric Framework for Simultaneous Non-Rigid Registration and Segmentation of Surfaces ⋆

N. Lord, J. Ho, and B.C. Vemuri
email: [nal, jho, vemuri]@cise.ufl.edu

UF-CISE Technical Report TR-06-001
Computer and Information Sciences Department
University of Florida
Bldg. CSE, Room 301
Gainesville, Florida 32611
April 18, 2006

⋆ This research was supported in part by the grant NIH-R01-NS04812 to BCV and the UF Alumni Fellowship to NAL. Data sets were provided by Dr. Christiana Leonard of the UF McKnight Brain Institute.

Abstract. In clinical applications where structural asymmetries between homologous shapes have been correlated with pathology, the questions of definition and quantification of 'asymmetry' arise naturally. When not only the degree but the position of deformity is thought relevant, asymmetry localization must also be addressed. Asymmetries between paired shapes can and have been formulated in the literature in terms of (non-rigid) diffeomorphisms between the shapes. For the infinity of such maps possible for a given pair, we define optimality as the minimization of total distortion, where 'distortion' is in turn defiend as deviation from isometry. We thus propose a novel variational formulation for segmenting asymmetric regions from surface pairs based on the minimization of a functional of both the deformation map and the segmentation boundary, which controls gradient discontinuity of the map. This minimization is achieved via a quasi-simultaneous evolution of the map and curve. Our formulation is inherently intrinsic and parameterization-independent. We present examples using both synthetic data and pairs of left and right hippocampal structures, hippocampus malformation being linked with such neurological disorders as epilepsy and schizophrenia.

1 Introduction

Many neurological disorders have been clinically correlated with shape abnormalities in specific brain structures. For example, hippocampal shrinkage is associated with epilepsy and schizophrenia, among other conditions. A precise analysis of such abnormalities, which are usually considered to be failures of symmetry of the left and right halves of the structure in question, could unlock the ability not only to track the progression of existent disease, but to identify at-risk individuals for preventative treatment. However, devising a framework in which to conduct the necessary shape comparison is a nontrivial matter. The shortcomings of raw volumetric comparison are obvious. Landmark-based methods are inapplicable to problems involving many anatomical structures (including the hippocampus), because many biological structures do not exhibit the sorts of readily and consistently identifiable local features on which such methods depend. The medial surface representation of Gerig et al. [1][2] represents a more sophisticated take on volumetric analysis that includes some localization of volume disparity, but the economy of the method leads both to noise sensitivity and an acknowledged inability to distinguish between different sorts of deformation (e.g. certain forms of elongation vs. bending). This is due to the expression of complicated behaviors in terms of simple distances which discard some amount of directionality.

More recently, Wang et al.[3][4][5] presented a technique involving the alignment of surfaces based on the formation of a 2D (parametric) diffeomorphic map from Riemannian surface structure information, with this map representing the non-rigid registration between the surfaces. This approach arguably makes use of what surface "feature" information is there to be had from relatively nondescript shapes, without imposing an ill-defined demand for landmark identification. However, in forming the correspondence by maximizing the mutual

information of the chosen surface characteristics over the entirety of both surfaces, these methods ignore key considerations. For one, while the conceptual division of the body into anatomical structures is hardly arbitrary in a general sense, for the purpose of deformation analysis, it may very well be. That is to say, we may wish to identify a selected portion of the hippocampus as structurally abnormal relative to its correspondent, rather than regarding the entire hippocampus as deformed. Furthermore, the MI of the domain and target surface features does not in and of itself restrict the differential properties of the map, only what properties should be found at given locations on the target surface. Therefore two regions of the target surface that exhibit the same Riemannian characteristics cannot be differentiated between, despite the fact that one choice may be physically unreasonable as a map target. Thus this framework demands a separate regularizing constraint on the map evolution.

To address these concerns, we present a novel approach to the non-rigid registration of anatomically correspondent surfaces which rests on the fundamental assumptions that (a) the relative deformity of anatomical structures for which symmetry is expected can be intuitively and precisely quantified as the deviation from isometry of the deformation map between their surfaces, and (b) since deformities may well be locally confined to certain regions of the given surfaces, the evolution of the global correspondence must allow for a partial disconnect between normal and abnormal regions, as these are by definition not expected to exhibit the same deformation patterns. As such, surface segmentation rests at the heart of our approach, which can be viewed not only as a registration tool but also as an asymmetry localizer and quantifier. Our definition of system energy in terms of isometry inherently balances the consideration that the map should accurately match Riemannian surface characteristics with the idea that the map should incur as little deformation as possible in doing so. This gives way to a simple, elegant formulation relatively free of heuristics. Since we here restrict our consideration to surfaces that are topologically cylindrical (appropriate for hippocampi among many other structures), we are able to parameterize with a single patch (periodic at a pair of ends) for each surface in the pair, and as the formulation is intrinsic, we can confine evolution to these 2D parametric domains, retaining elegance. The evolution is driven quasi-simultaneously by the energies of both the segmenting curve and the deformation field, in the spirit of the works of Yezzi et al. and Unal et al.[6][7], where the former group restricted its work to rigid image registration and the latter generalized the idea to the non-rigid deformation case. In [8], Vemuri et al. presented a registration-assisted image segmentation technique. Of the many proposals in the literature which followed, however, none addressed the issue of joint manifold segmentation and registration, which is our focus. Our work differs notably in that we evolve the segmenting curve and the registration map on a general 2D manifold (rather than a flat image plane), and rather than registering and segmenting image data, we register and segment the shape characteristics of the very surface on which the processes are operating.

The rest of the paper is organized as follows: Section 2 contains the mathematical formulation and numerical algorithm used to solve it. Section 3 contains experimental results on both synthetic and real data sets. In section 4, we draw conclusions.

2 Simultaneous Segmentation and Registration Algorithm

Let $\mathbf{S}_1$ and $\mathbf{S}_2$ be two surfaces in $\mathbb{R}^3$. The Euclidean metric in $\mathbb{R}^3$ induces Riemannian metrics g_1 and g_2 on $\mathbf{S}_1$ and $\mathbf{S}_2$, respectively. The goal of the algorithm is to segment regions in $\mathbf{S}_1$ and their corresponding regions in $\mathbf{S}_2$ such that the metric structures of the corresponding regions match optimally. More specifically, the algorithm computes a homeomorphism f between $\mathbf{S}_1$ and $\mathbf{S}_2$ **and** a set of closed curves γ_1 on $\mathbf{S}_1$. Let γ_2 denote the closed curve in $\mathbf{S}_2$ that is the image of γ_1 under f. The restriction of f to the complement $\mathbf{S}_1\backslash\gamma_1$ is a diffeomorphism between $\mathbf{S}_1\backslash\gamma_1$ and $\mathbf{S}_2\backslash\gamma_2$. If $U_1, \cdots, U_n$ and $V_1, \cdots, V_n$ denote the collections of open components of $\mathbf{S}_1\backslash\gamma_1$ and $\mathbf{S}_2\backslash\gamma_2$, respectively, then f maps U_i diffeomorphically onto V_i for each i and f matches the Riemannian structures between that of U_i and of $V_i = f(U_i)$. See Figure 1. We solve the simultaneous

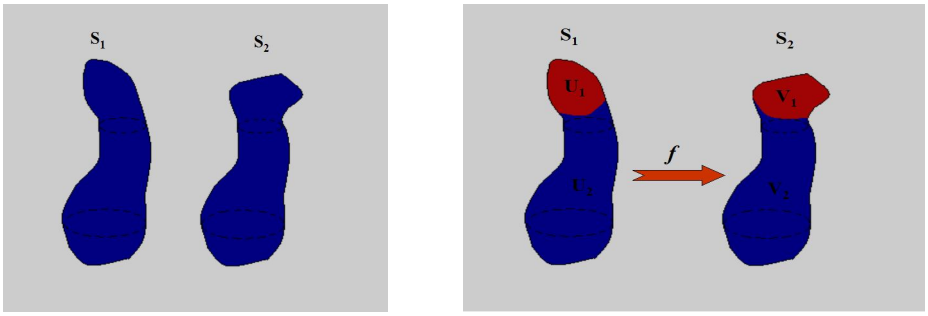

Fig. 1. Left: The two given surfaces, $\mathbf{S}_1$ and $\mathbf{S}_2$. **Right:** The desired result of simultaneous segmentation and registration of these two surfaces. The map f is a homeomorphism between $\mathbf{S}_1$ and $\mathbf{S}_2$. f maps the segmenting curve γ_1 on $\mathbf{S}_1$ to a curve γ_2 on $\mathbf{S}_2$, and f establishes correspondences between connected components of $\mathbf{S}_1\backslash\gamma_1$ and $\mathbf{S}_2\backslash\gamma_2$. U_1 and U_2 are two disjoint open sets in $\mathbf{S}_1\backslash\gamma_1$, and V_1 and V_2 are two disjoint open sets in $\mathbf{S}_2\backslash\gamma_2$. f maps U_i diffeomorphically onto V_i for each i. The restriction of f to U_i optimally matches the Riemannian structures of U_i and V_i.

segmentation and registration problem outlined above using a variational framework. The energy functional $\mathcal{E}$ is defined as a functional of a pair (f, γ_1), where γ_1 is a set of closed curves on $\mathbf{S}_1$ and $f : \mathbf{S}_1 \rightarrow \mathbf{S}_2$ is a homeomorphism which is C^∞ on $\mathbf{S}_1\backslash\gamma_1$. Let f^*g_2 denote the pull-back metric (the first fundamental form)

on g_1, and $\mathcal{E}(f,\, \gamma_1)$ is defined as

$$\mathcal{E}(f,\, \gamma_1) = \int_{\mathbf{S}_1 \setminus \gamma_1} |f^* g_2 - g_1|^2 dA + \int |df(\gamma_1(t))/dt|_{g_2} dt. \tag{1}$$

The second integral computes the length of the segmenting curve γ_2 on $\mathbf{S}_2$, while the first integral computes the matching (registration) cost between the two Riemannian structures on the complement, $\mathbf{S}_1 \setminus \gamma_1$. By computing the length of the segmenting curve on $\mathbf{S}_2$ instead of $\mathbf{S}_1$, the energy functional tightly couples the two somewhat disparate processes, segmentation and registration. The integrand of the first term above, $|f^* g_2 - g_1|^2$, is the usual L^2-norm between the two tensors g_1 and $f^* g_2$. In local coordinates, it is given as the usual L^2-norm between the two matrices G_1 and $J^t G_2 J$:

$$|J^t G_2 J - G_1|^2_{g_1}, \tag{2}$$

where J is the Jacobian of f expressed in the local coordinates system, and G_1 and G_2 are the usual 2×2 positive definite matrices expressing the metric tensors g_1 and g_2 in the given local coordinates on $\mathbf{S}_1$ and the induced one (using f) on $\mathbf{S}_2$.

At this point, a comparison between our approach and the usual Mumford-Shah framework [9] is called for. Given an image I, the energy functional for Mumford-Shah is

$$\mathcal{MS}(I'\ \gamma) = \int_{\mathcal{D}} |I - I'|^2 dA + \int_{\mathcal{D} \setminus \gamma} |\nabla I'|^2 dA + \int |\gamma'(t)| dt.$$

In the above, $\mathcal{D}$ denotes the image and γ the segmenting curve on $\mathcal{D}$. The third term, which measures the length of γ, corresponds directly to the second term of $\mathcal{E}$ in 1. The first two terms of Mumford-Shah, representing data fidelity and smoothness, respectively, may seem to lack analogous entries in $\mathcal{E}$. However, we argue below that the first integral in the definition of $\mathcal{E}$ serves both as the fidelity and smoothing term for $\mathcal{E}$, and we can thus consider $\mathcal{E}$ as a generalization of the usual Mumford-Shah functional to the problem of simultaneous shape registration and segmentation.

For our problem, we want to *compare* two surfaces $\mathbf{B}_1$ and $\mathbf{B}_2$ via their respective Riemannian structures g_1 and g_2, and to extract a meaningful segmentation from the comparison. Instead of an image I' as in the usual Mumford-Shah framework, our variable is the map f between $\mathbf{S}_1$ and $\mathbf{S}_2$. In our case, the data fidelity requirement appears as the penalization of f for failure to match the Riemannian structures of the surfaces, while the smoothing term appears as the penalization of f for large first-order derivative magnitudes. A close examination of Equation 1 reveals that the first integral indeed contains both requirements. First, the norm between the two tensors $f^* g_2$ and g_1 as defined in Equation 2 clearly measures the quality of match between the two metric tensors. Second, the Jacobian J contains all of the first-order derivatives of f, and the squared-norm in Equation 2 indirectly measures the magnitudes of the

first-order derivatives of f using both metrics g_1 and g_2. In sum, we can interpret the first term in Equation 1 as the integration of the first two terms in the usual Mumford-Shah functional $\mathcal{MS}$. In $\mathcal{MS}$, these two terms are necessarily separate because there is no natural connection between matching pixel intensities and restricting the gradient ∇I. In our problem, the connection between matching and smoothing is natural: since we are matching Riemannian structures, which are tensors defined on tangent spaces, any matching between these two structures has to involve some kind of (implicit) matching between tangent spaces, and the appearance of derivatives in defining the matching is then unavoidable.

2.1 Minimizing the Energy Functional $\mathcal{E}$

In implementing the energy minimization as defined above, we rely on alternating iterations between a Chan-Vese level set curve segmenter [10], extended to the general 2D manifold domain, which produces a step towards the best estimate of the segmentation of the energy field given the current map, and a sparse Hessian-exploiting quasi-Newton optimization scheme acting on the non-rigid map between the parametric domains, which provides a step towards the minimum-energy map between the surfaces as constrained by the current position of the segmenting curve. The manner in which the curve separates the evolution occurring on its exterior from that occurring on its interior relates to a Neumann condition imposed across the boundary, akin to what is suggested in the Mumford-Shah curve evolution implementation in [11]. The curve length minimizing term implementation is straightforward, though curvature computation must take nonuniform surface length elements into account. Hippocampus surface data used in this investigation was brought into rigid alignment by ICP in a preprocessing step, then 2D sliced and manually segmented by a trained neuro-anatomist into a 40x21 grid periodic in one direction. This grid in effect forms a parametric domain for the corresponding surface, and the Riemannian surface characteristics are thus calculated by numerical methods and stored in said domain.

3 Results

We here present examples of the algorithm in action, validating its behavior on synthetic cases and demonstrating results obtained on real hippocampus pairs. As a starting point, we consider the trivial case of a pair of cylinders, where one member of the pair has had its surface distorted according to an outward normal vector field of magnitude dictated by a Gaussian distribution. That is to say, its surface has been bumped. In Fig. 2, we see a comparative case involving a cylinder with two such distortions versus its unaltered counterpart. The intuition behind our method asserts that we should "blame" the applied bumps for observed differences between the Riemannian surface characteristics of the two shapes. Obviously, then, the desired result is the segmentation of the two clearly visible bumps on the left cylinder, which is what we observe. (Red

'hot spots,' the curve interiors, represent regions of highest deformation energy under the current map and segmentation. The curve itself is found at the border between the red and blue regions.) Note the textured quality of the surfaces, which occurs as a result of the addition of a SD=0.02 zero-mean Gaussian noise field to the (X,Y,Z) coordinates of the (unit radius) cylinders prior to output, for demonstration of robustness in the face of noise in surface scanning.

As indicated previously, the case of the cylinder is a trivial one in this context in that there exists a "natural" parameterization of the surface which results in a constant metric tensor field over the parametric domain. Thus, we further validate using synthetic alterations to real data exhibiting arbitrary shape, within the confines of cylindrical topology. Since the hippocampus meets these criteria and forms part of our clinical motivation, it seems a natural choice. Selecting a single hippocampal horn, we again apply a small outward normal Gaussian deformation to its surface, whose location we hope to see the segmenter recover. However, rather than illustrating invariance to surface point cloud noise, we now seek to additionally validate invariance of the solution to reparameterizations of the given surfaces. To pause for conceptual refreshment, recall that in comparing surfaces we are in fact comparing two parametric domains based on the two tensor-valued functions corresponding to each of those domains, those functions being the Riemannian surface structure information of each parameterized surface. But just as two surfaces (or their parametric domains, as we do in our implementation) can be mapped to one another nonrigidly in infinitely many ways, so too can each parametric domain map to its topologically-equivalent parameterized surface in infinitely many ways. The Riemannian structure tensor fields themselves depend upon which of these infinitely many parameterizations are chosen. When synthetically producing one surface from another, we possess a trivial alignment between the domains under which the two tensor fields are identical, excepting the patch corresponding to the synthetic bump. In real cases, of course, data will not have this sort of property. The validation is thus incomplete until we can show that under a suitably deformed reparameterization of one of the surfaces being compared, a result comparable to the above is achieved. We can reparameterize simply by randomly generating a distortion of the parametric domain's regular grid, then interpolating a new point cloud from the given data based on the new locations of the gridpoints. It is completely appropriate to confine said distortion to the order of a pixel in each direction: after all, we have assumed close rigid alignment and sensibly spaced data points from our preprocessing, and if these constraints are violated, they can always be reinstated by repeating the algorithms that enforced them in the first place. The purpose of the nonrigid registration evolution is to further refine the surface correspondence following bulk rigid alignment of the shapes based on the surface characteristics observed locally, not to register raw point clouds. We cannot show the parameterization warp used due to space constraints: it is of 0.1 SD in each coordinate.

It is visually evident that the segmentation succeeds despite the change of parameterization of one of the surfaces being compared. The deformation map

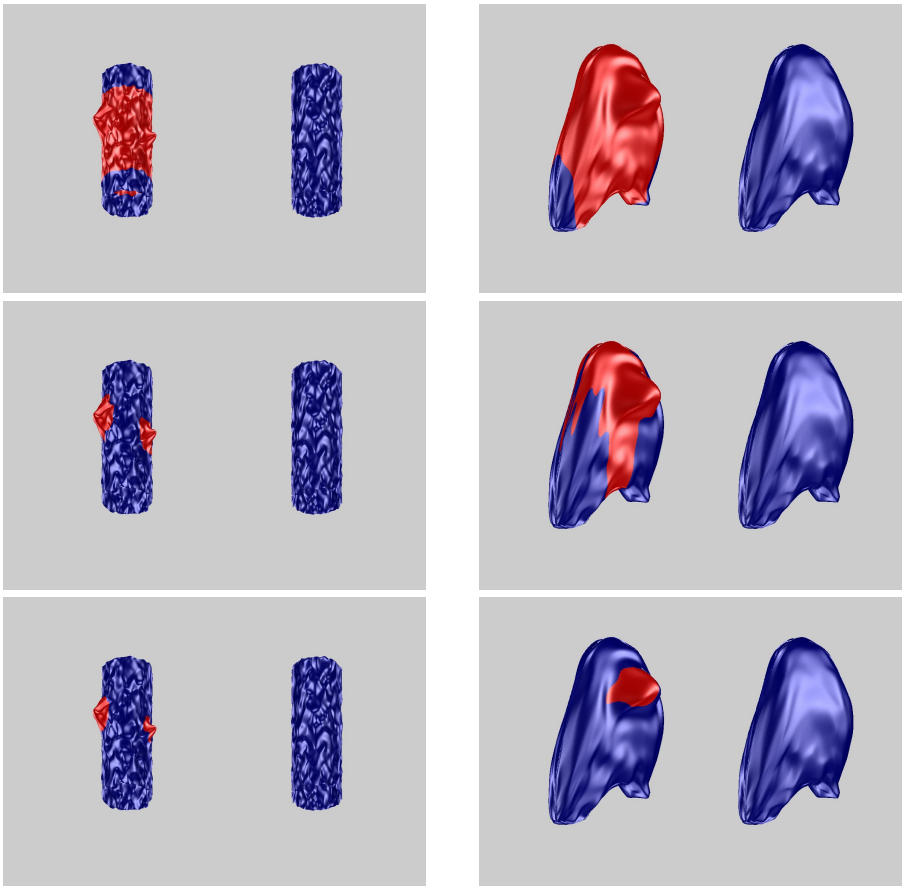

Fig. 2. Left column: Segmentation of prominent distortions (bumps) from cylindrical surface, based on comparison to homologous cylinder lacking bumps. Surfaces are both distorted with distinct random noise fields (seen as textured effect). Top: naive initialization; Middle: 3 iterations; Bottom: 10 iterations. **Right column:** Segmentation of synthetic bump from surface of real hippocampus, based on comparison to same hippocampus without bump. The two hippocampi are under different parameterizations. Top: naive initialization; Middle: 5 iterations; Bottom: 20 iterations.

between the parametric domains (not shown) undergoes considerable evolution through this process. This evolution can be best understood as the method's attempt to invert the reparameterization, to achieve the optimal alignment of the identical surface patches external to the segmented bump, while at the same time trying to find the minimum energy description of the acknowledged deformation of the patch on the curve's interior.

In presenting the following real example, we issue the caveat that the method's success lies in the eye of the beholder, because there is of course no ground truth associated with this sort of problem. For this reason we have selected a case with an "answer" which can easily be agreed upon. Fig. 3 shows the left and right hippocampi clinically segmented from an MRI scan of an epilepsy patient. We take it as self-evident that there exists a localizable region of high distortion between the left and right shapes, and assume that one will agree that our method has in fact converged to a segmentation of that region. Illustrations of the segmented energy field and parametric warp evolutions have been withheld due to space limitations.

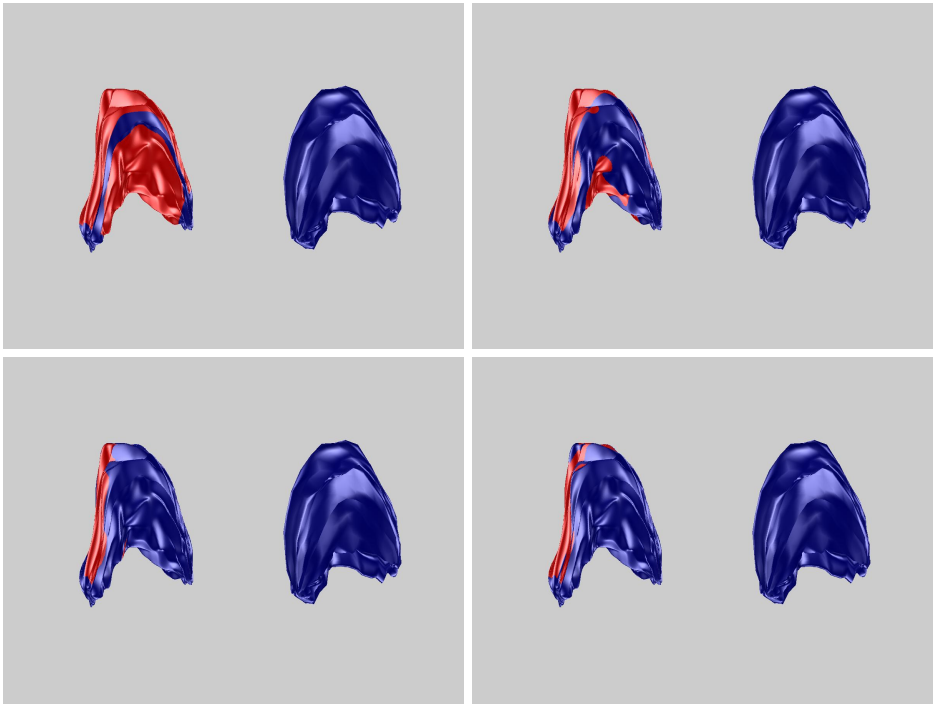

Fig. 3. Segmentation of distortion between real hippocampi of epileptic. Top left: naive initialization; Top right: 1 iteration; Bottom left: 5 iterations; Bottom right: 20 iterations.

4 Conclusion

We have presented a novel scheme for simultaneous nonrigid registration and segmentation of homologous shapes, wherein the interdependent registration and segmentation processes are driven by intrinsic geometric characteristics of the shapes themselves. As such, we are able not only to identify surface pairs representing large deformations, but also to specify which subregions of the shapes appear most likely to be involved in the deformation, to produce an estimate of the implicit deformation field, and to quantify the deformation energy of the segmented subregions separately from that of the remaining surface patches. Given the number of considerations interplaying, the variational principle driving the evolution is notably compact. We have seen that the method's results are reasonably invariant to local parameterization changes and added surface noise, and results on real data (while inherently lacking in ground truth for comparison) appear promising. Future efforts could include the application of the method to extensive real datasets that have been clinically preclassified according to the presence or absence of pathology, as well as an attempt to correlate the locations and intensities of the segmented deformed regions with the given pathology classifications. It should also be noted that the two-region Chan-Vese segmentation method (which is often used for its strong balance of effectiveness and relative simplicity of implementation) is merely a good "first draft" of a segmentation scheme for this sort of problem. A more robust segmentation method, such as the general Mumford-Shah functional extended to arbitrary surfaces, would doubtless prove beneficial, as our energy fields will not always neatly obey the two-mean framework. Finally, it goes without saying that all evolution/optimization-based methods (apart from the most trivial cases) suffer from some amount of initialization-dependence. Intelligent initialization schemes could be expected to further boost performance.

References

1. Gerig, G., Muller, K.E., Kistner, E.O., Chi, Y.Y., Chakos, M., Styner, M., Lieberman, J.A.: Age and treatment related local hippocampal changes in schizophrenia explained by a novel shape analysis method. In: MICCAI. (2003) 653–660
2. Styner, M., Lieberman, J.A., Gerig, G.: Boundary and medial shape analysis of the hippocampus in schizophrenia. In: MICCAI. (2003) 464–471
3. Wang, Y., Gu, X., Hayashi, K.M., Chan, T.F., Thompson, P.M., Yau, S.T.: Surface parameterization using riemann surface structure. In: Proc. Int. Conf. on Computer Vision. (2005) 1061–1066
4. Wang, Y., Chiang, M.C., Thompson, P.M.: Mutual information-based 3d surface matching with applications to face recognition and brain mapping. In: Proc. Int. Conf. on Computer Vision. (2005) 527–534
5. Wang, Y., Chiang, M.C., Thompson, P.M.: Automated surface matching using mutual information applied to riemann surface structures. In: MICCAI. (2005) 777–674
6. A.Yezzi, Zollei, L., Kapur, T.: A variational framework for joint segmentation and registration. In: CVPR - MMBIA. (2001)

7. Unal, G.B., Slabaugh, G.G.: Coupled pdes for non-rigid registration and segmentation. In: CVPR. (2005) 168–175
8. Wang, F., Vemuri, B.C.: Simultaneous registration and segmentation of anatomical structures from brain mri. In: MICCAI. (2005) 17–25
9. Mumford, D., Shah, J.: Optimal approximations by piecewise smooth functions and associated variational problems. Commun. Pure Appl. Math **42**(4) (1989)
10. Chan, T.F., Vese, L.A.: Active contours without edges. IEEE Transactions on Image Processing **10**(2) (2001) 266–277
11. Tsai, A., Yezzi, A.J., Willsky, A.S.: Curve evolution implementation of the mumford-shah functional for image segmentation, denoising, interpolation, and magnification. IEEE Transactions on Image Processing **10**(8) (2001) 1169–1186